



# A DCT-JND Profile for Disorderly Concealment Effect

Hongkui Wang<sup>1</sup>, Li Yu<sup>1</sup>(✉), Tiansong Li<sup>1</sup>, Mengting Fan<sup>2</sup>,  
and Haibing Yin<sup>3</sup>

<sup>1</sup> School of Electronic Information and Communications,  
Huazhong University of Science and Technology, Wuhan, China  
{hkwang, hustlyu}@hust.edu.cn

<sup>2</sup> College of Information Engineering,  
China Jiliang University, Hangzhou, China

<sup>3</sup> School of Communication Engineering, Hangzhou Dianzi University,  
Hangzhou, China

**Abstract.** Just noticeable distortion (JND) refers to the smallest visibility threshold of the human visual system (HVS). The existing JND profiles always overestimate the visibility threshold in orderly region and underestimate that of the disorderly region. In order to obtain a more accurate DCT-JND profile, a novel block-level disorder metric is proposed and disorderly concealment effect is taken into account in the DCT-JND model. Specifically, an improved perceptive Local Binary Patterns (LBP) algorithm is proposed to evaluate the disorder of each block in this paper. Since the visual acuity is insensitive to the disorder stimulus, a disorderly concealment effect factor is defined as the function of block disorder and background disorder in this paper. The factor is used to adjust the conventional JND threshold appropriately. The experimental result shows that the proposed JND model tolerates much more distortion with the same perceptual quality compared with the existing JND profiles.

**Keywords:** Disorderly concealment effect · Block-level disorder metric  
DCT-JND model

## 1 Introduction

The human visual system perceives the pixel change above a certain visibility threshold. The minimal visibility threshold is called the just noticeable distortion. Exposing the perceived characteristics of HVS, the JND profile has been adopted in many image and video processing fields such as image/video compression [1], quality assessment [2], scene enhance [3], etc.

In general, the JND profile is divided into pixel-based and subband-based (e.g., DCT, DFT) JND models. Because most of image and video compression schemes are performed in DCT domain, the DCT-JND model attracts many researchers' attention. In 1192, Ahumada and Peterson [4] proposed the first DCT-JND model which gives the JND threshold for each DCT component. The threshold is determined by the spatial contrast sensitivity function (CSF) which is used to describe the band-pass property of

sensitivity of HVS in spatial frequency. DCTune [5] is an improved model proposed by Watson, in which the luminance adaptation (LA) effect and the contrast masking (CM) effect had been incorporated. The LA effect indicates that the visual sensitivity is low in the dark and light regions. As for the CM effect, it is referred to as the reduction in the visibility of one visual component in the presence of another. In conventional DCT-JND model, the edge pixel density calculated by the Canny operator is employed to evaluate the contrast intensity of each block [6]. By calculating the standard deviation of pixels and the power spectrum density of each frequency, Bae recently proposed the structural contrast index (SCI) metric to evaluate the contrast intensity of DCT blocks [7]. Although it was reported that the SCI metric describes the block contrast accurately and effectively, the contrast intensity of edge regions calculated by SCI metric is always higher relatively. In fact, the existing JND profiles mainly consider the LA and CM effects, which always overestimates the visibility threshold of the edge region and underestimates that of the texture region [8].

In order to overcome the aforementioned limitation of JND models, some literatures had made meaningful explorations to improve the accuracy of JND models. Wu et al. [9] divides the image into orderly image and disorderly image with an autoregressive model. The disorderly concealment effect was taken into account in pixel-JND model at the first time. Disorderly concealment effect reveals that HVS is sensitive to the orderly stimulus but tries to avoid uncertainties caused by disorderly information. Recently, the pattern masking based on both CM effect and structural uncertainty was introduced in [8]. Due to the masking is determined by both luminance contrast and pattern complexity, it is limited in regular pattern and is strong in irregular pattern. It was reported that the JND model considering pattern masking is more consistent with the HVS than other JND models. However, these models are constructed in pixel domain and can't be applied in DCT domain directly.

As an extension of Wu's model [8], a disorderly concealed effect factor is proposed to adjust the conventional DCT-JND threshold appropriately. Since the visual acuity is insensitive to disorderly stimulus, the factor is defined as a function of the block disorder and the background disorder. The disorder of each block is evaluated by an improved perceptive LBP algorithm in this paper. Experimental results confirm that the proposed model tolerates much more distortion with the same perceptual quality compared with the existing JND profiles.

## 2 The Proposed DCT-JND Model

### 2.1 Conventional DCT-JND Model

The conventional DCT-JND model is expressed as a product of three modulation factors:  $J_{base}$  is applied to measure the JND threshold for each spatial frequency component.  $F_{LA}$  and  $F_{CM}$  are LA and CM effect factors.

$$J(N, \omega, n, i, j, \tau) = J_{base}(N, \omega) \cdot F_{LA}(n) \cdot F_{CM}(\omega, \tau) \quad (1)$$

Here,  $n$  is the block index and  $(i, j)$  is the DCT coefficient index. Ordinarily, human eyes are sensitive to the horizontal and vertical frequency and insensitive to the diagonal components. Considering the spatial summation effect [10] and oblique effect [10], the  $J_{base}$  of each DCT coefficient is modified as

$$J_{base}(i, j) = N \cdot F_s \cdot \exp(c\omega_{ij}) / (a + b\omega_{ij}) / [(r + (1 - r) \cdot \cos^2 \varphi_{ij})] \quad (2)$$

where  $N$  is DCT normalization factor for an  $N \times N$  DCT block.  $\omega_{ij}$  is the corresponding frequency of  $(i, j)$ -th subband in DCT block.  $F_s$  is spatial summation effect factor and takes the value of 0.125 [7]. The parameters are set  $a = 1.33$ ,  $b = 0.11$ ,  $c = 0.18$ ,  $r = 0.6$  according to Wei's psychophysical experiments [10]. In term  $r + (1 - r) \cdot \cos^2 \varphi_{ij}$  accounts for the oblique effect and  $\varphi_{ij}$  equals to  $\arcsin(2 \cdot \omega_{i,0} \cdot \omega_{0,j} / \omega_{ij}^2)$ . Due to the SCI metric has better performance in contrast measurement, we adopt Bae's CM effect factor [7] in our DCT-JND model. The LA and CM factors are computed by formula (3) and (4).

$$F_{LA}(n) = \begin{cases} (60 - I(n))/150 + 1 & I \leq 60 \\ 1 & 60 < I \leq 170 \\ (I(n) - 170)/425 + 1 & I > 170 \end{cases} \quad (3)$$

$$F_{CM} = f(\omega) \cdot \tau \cdot \varepsilon + 1 \quad (4)$$

where  $I(n)$  is the average intensity value of the  $n$ -th block.  $f(\omega)$  is the gain function of spatial frequency.  $\varepsilon$  is an invariant constant which is equal to 0.2.  $\tau$  is the contrast intensity of the DCT block which is equal to  $C_t^\alpha / K_t^\beta$ .  $C_t$  represents the contrast intensity that can be calculated by the Parseval's theorem. The  $K_t$  is the Kurtosis of normalized power spectral density of DCT coefficients.  $\alpha$ ,  $\beta$  are the paraments that are empirically set to 1.4 and 0.7.

## 2.2 Considerations for the Improvement of the DCT-JND Model

The relationship between the contrast intensity ( $\tau$ ) and edge pixel density ( $\rho$ ) of each block is shown in Fig. 1. The block is divided into three types (i.e., plain, edge and texture) according to the edge pixel density [9]. As shown in Fig. 1, compared with other regions, the contrast intensity in edge region is higher relatively. Nevertheless, noise is easily observed in the smooth and edge areas. Therefore, the conventional DCT-JND model always overestimates the visibility threshold of the edge region and underestimates that of the texture region [8].

Recent research on human perception indicates that the HVS possesses an internal generative mechanism (IGM) for visual signal processing. The IGM theory suggests the visual acuity is sensitive to the orderly region and is insensitive to the disorderly region [11]. For applying the perceived characteristic of HVS effectively, the disorderly concealed effect should be properly incorporated into the DCT-JND model. How to efficiently incorporate the disorderly concealed effect into DCT-JND model is an open problem. In this paper, a disorderly concealed effect factor is designed to adjust the conventional DCT-JND threshold. Since the visual acuity is insensitive to the

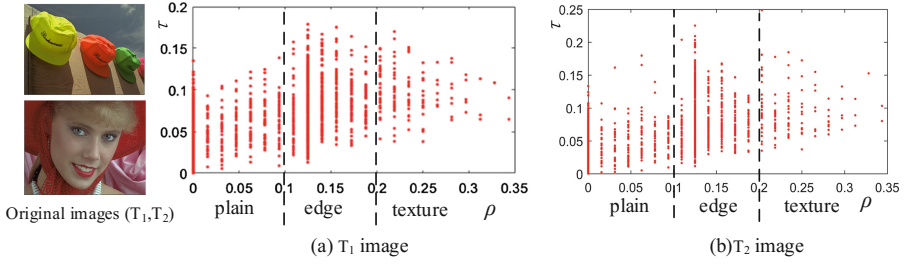


**Fig. 1.** The relationship between contrast intensity ( $\tau$ ) and the edge pixels density ( $\rho$ ).

disorderly stimulus, the factor ( $F_{DC}$ ) can be defined as a function of the block disorder ( $\xi_{block}$ ) and the background disorder ( $\xi_{back}$ ) based on the psychophysical experiments. In DCT domain, the block is the image processing unit. Therefore, a block-level disorder metric is designed to evaluate the disorder of the block. Therefore, the total DCT-JND can be written by

$$J(N, \omega, n, i, j, \tau) = J_{base}(N, \omega) \cdot F_{LA}(n) \cdot F_{CM}(\omega, \tau) \cdot F_{DC}(\xi_{block}, \xi_{back}) \quad (5)$$

### 3 The Block-Level Disorder Metric

The visual acuity is sensitive to the orderly stimulus and is insensitive to the disorderly stimulus [11]. In order to evaluate the disorder intensity of the stimulus, a block-level disorder metric is introduced in this section.

Ojala et al. [12] analyzed the spatial relationship among pixels and introduced a classic LBP algorithm to describe the orderly information of each pixel. In particular, for an  $N \times N$  block, the orderly information of the intermediate pixel ( $x_c$ ) is represented by the relationship between the  $x_c$  and the adjacent pixels  $x_i$ . The block size  $N$  is always set as 3 by considering the accuracy and computational complexity. The LBP value of  $x_c$  is expressed as

$$LBP(x_c) = \sum_{i=1}^N t(x_i - x_c) \times 2^{i-1} \text{ and } t(x_i - x_c) = \begin{cases} 1, & x_i \geq x_c \\ 0, & x_i < x_c \end{cases} \quad (6)$$

where  $t$  is the sign of differences between the pixel  $x_c$  and  $x_i$ . Wu et al. [8] considered the LA effect and proposed a perceptive LBP algorithm based on a luminance adaptive threshold. The luminance adaptive threshold is expressed by formula (7).  $I(x_c)$  is the average background luminance intensity of pixel  $x_c$ .

$$LA(x_c) = \begin{cases} 17 \times (1 - \sqrt{I(x_c)/127}), & \text{if } I(x_c) \leq 127 \\ 3/128 \times (I(x_c) - 127) + 3, & \text{else} \end{cases} \quad (7)$$

However, Wu's LBP algorithm is used to evaluate the orderly information of each pixel and can't be used in block-level disorder evaluation directly. In order to estimate the disorder of the block with different dimensions, an improved perceptive LBP algorithm is proposed. For the sake of simplicity, the example of calculation process with  $N = 8$  is shown in Fig. 2. As shown in Fig. 2(a), four directions (i.e.,  $D_0, D_1, D_2, D_3$ ) are considered in an  $N \times N$  block (e.g.,  $N = 8$ ) and the pixels which are applied to calculate the orderly information are defined. Due to the dimension of block is always even, there are two row pixels and two column pixels to be used in horizontal and vertical directions. Therefore, six computing patterns (i.e.,  $P_0, P_1, \dots, P_5$ ) are designed in four directions. There are two patterns in horizontal and vertical directions respectively. For the convenience of description, the pixels in each pattern are defined  $x_0$  to  $x_7$  as Fig. 2(b). The sign of differences of each pattern is expressed as

$$t_{ik} = \begin{cases} 1, & x_{ik} - x_{ik-1} \geq LA(x_{ik-1}) \\ 0, & |x_{ik} - x_{ik-1}| < LA(x_{ik-1}) \\ -1, & x_{ik} - x_{ik-1} \leq -LA(x_{ik-1}) \end{cases} \quad (8)$$

where  $k$  is the index of the pattern (i.e.,  $k = 0, 1, 2, \dots, 5$ ).  $i$  is the pixel index in each pattern. The LBP value of each pattern is calculated by

$$\zeta_k = \sum_{i=0}^7 |t_{ik}| \times 2^{q(ik)} \quad (9)$$

$2^{q(ik)}$  is the weight function. Human eyes pay more attention to the center of the stimulus because of the center prior principle. The visual weight increases when the distance between the current  $t_{ik}$  and the center one decreases in each pattern. The disorder intensity is related to the number of continuous unequal  $t_{ik}$  in each pattern.

$$q(i) = \begin{cases} 0, & i = 0 \text{ or } i = 7 \text{ or } t_i = t_{i-1} \\ q_{i-1} + 1, & t_i \neq t_{i-1} \text{ and } i < 4 \\ q_{i+1} + 1, & t_i \neq t_{i+1} \text{ and } i \geq 4 \end{cases} \quad (10)$$

$q(i)$  represents the number of continuous unequal  $t_i$ . The underlying idea of Eq. (10) is that the larger of  $q(i)$ , the disorder is much stronger. An example of  $t_{ik}$  is shown in Fig. 2(c). At last, for the sake of discussion without losing its generality, the block-level disorder is calculated by formula (11).  $w_k$  is the weight of  $k$ -th pattern. Considering the oblique effect, the weights in horizontal diagonal direction (i.e.,  $w_2, w_5$ ) are equal to 1.67. The weights in other directions (i.e.,  $w_0, w_1, w_3, w_4, w_6$ ) are equal to 1.0 [10].  $\zeta_{\max}$  is the normalization factor and is set to 151. Figure 3 shows the block-level disorder intensity of images. Higher brightness means a larger disorder value. It is obvious that the block in disorderly region has high disorder value in Fig. 3.

$$\zeta_{\text{block}}(n) = \sum_{k=0}^5 \zeta_i \cdot w_k \Big/ \zeta_{\max} \quad (11)$$

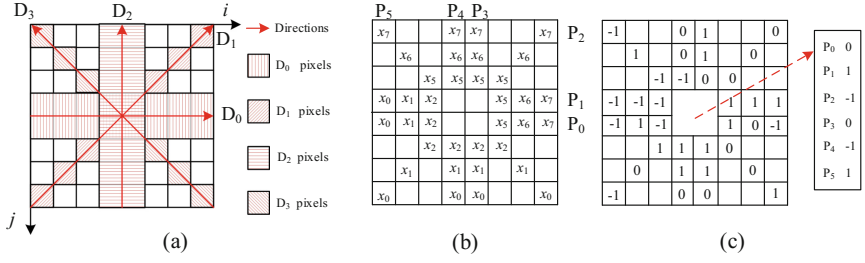


**Fig. 2.** The calculation process of the improved perceptive LBP algorithm: (a) four directions; (b) six computing patterns; (c) the sign of differences.

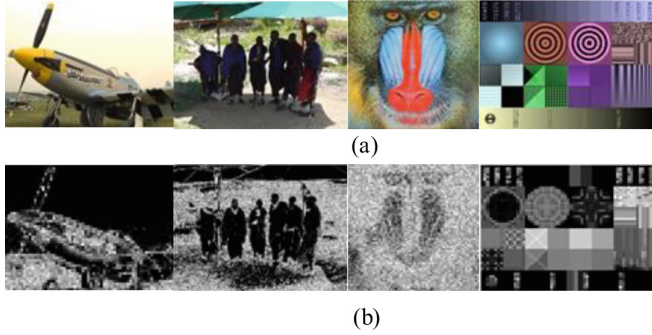


**Fig. 3.** The block-level disorder: (a) the original images; (b) the disorder map.

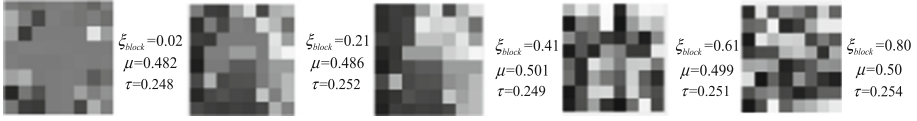
## 4 The Disorderly Concealment Effect Factor

The sensitivity of HVS is related to the block disorder ( $\xi_{block}$ ) and the background disorder ( $\xi_{back}$ ). The background disorder is defined as the average disorder intensity of the background. In order to measure the disorderly concealment effect of block and background to human visual acuity, we perform the psychophysical experiment for DCT-JND measurement. The test conditions for our psychophysical experiments are summarized in Table 1. For the background disorder of test stimulus, 5 test background disorder values are set to 0, 0.2, 0.4, 0.6 and 0.8. In only considering the disorderly concealment effect process, the LA and CM effects should be eliminated. According to the analysis in Sect. 2, The LA and CM effects of the block are related on the average intensity ( $I(n)$ ) and the contrast intensity ( $\tau$ ) [7]. Therefore, the test patches are designed as shown in Fig. 4.  $\mu$  is the normalized value of  $I(n)$  and is set to 0.5 approximately. The contrast intensity ( $\tau$ ) is 0.25 approximately.

The test example is shown in Fig. 5. As shown in Fig. 5(a), the test patch and test background are set in the center of the real background. Figure 5(b) represents the test image in DCT domain and shows the noise injected into  $R_1$ . The amplitude of noise in  $R_1$  increases until testers perceive the resulting distortion called the JND measured value. Each measured JND value is the value that 50% of the testers start to perceive

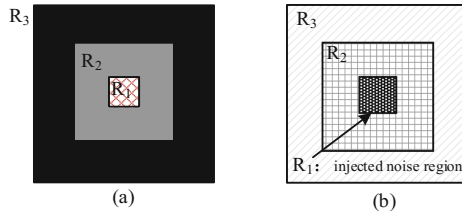
**Table 1.** Experimental setup

Display information	SONY KD-55X8000E (LED 55 inch, Full-HD resolution)
Viewing distance	1.75 times Screen height ( $\approx 1.2$ m)
Test patch ( $R_1$ )	$8 \times 8$ pixels (square blocks)
Test background ( $R_2$ )	$24 \times 24$ pixels (square blocks)
Real background ( $R_3$ )	$256 \times 256$ pixels

**Fig. 4.** The test patches with different block disorder ( $\xi_{block}$ ).

the corresponding distortions [7]. The measured disorderly concealment effect factor is represented by  $F_{DC}^*$  and the measured JND threshold is represented by  $J^*$ . As shown in Eq. (5), the  $F_{DC}^*$  is defined as a multiplier in our total DCT-JND model. Therefore, the  $F_{DC}^*$  is obtained by

$$F_{DC}^*(\xi_{block}, \xi_{back}) = \frac{J^*(\omega, n, N, \tau, \xi_{block}, \xi_{back})}{J^*(\omega, n, N, \tau, \xi_{block} = 0, \xi_{back} = 0)} \quad (12)$$

**Fig. 5.** A test image example: (a) the test patch and test background in the center of the real background; (b) the injected noise at the test patch in DCT domain.

It is known that the visual sensitivity to distortions decreases as the disorder intensity increases. In JND modelling, this indicates that the disorderly concealment effect factor ( $F_{DC}$ ) can be modeled as a monotonically increasing function for the block disorder ( $\xi_{block}$ ) and background disorder ( $\xi_{back}$ ). The test results are shown in Fig. 6. It is observed that the measured disorderly concealment effect ( $F_{DC}^*$ ) values increase approximately in an exponential manner as the block disorder for the given background disorder in Fig. 6(a). In Fig. 6(b), the measured ( $F_{DC}^*$ ) values increase approximately in a linear manner as the background disorder for the given block disorder. The relationship between the measured  $F_{DC}^*$  values and the different combinations of block disorder and background disorder is shown in Fig. 6(c).

Based on the observations in Figs. 6(a, b), we projected the  $F_{DC}^*$  values onto the two parameter spaces of the block disorder and the background disorder. The linear model is adopted to model the  $F_{DC}$ .

$$F_{DC} = \Psi(\xi_{back}) \cdot \Phi(\xi_{block}) + \eta \quad (13)$$

$\Phi(\xi_{block})$  is an exponential function to represent that disorderly concealment effect factor ( $F_{DC}$ ) increases as the block irregularity increases.  $\Psi(\xi_{back})$  is the weight of the exponential function and is modeled as a function of background disorder.  $\eta$  is the basis and is set to  $-0.25$ , empirically. The factor is constructed based on the least mean square as shown in Fig. 6(d).  $\Phi(\xi_{block})$  and  $\Psi(\xi_{back})$  are expressed with  $\eta_1 = 20$ ,  $\eta_2 = 40$ ,  $\eta_3 = 0.8$ ,  $\eta_4 = 0.4$ ,  $\eta_5 = 1$ .

$$\Phi(\xi_{block}) = \eta_1^{\xi_{block}/\eta_2} + \eta_3 \quad (14)$$

$$\Psi(\xi_{back}) = \eta_4 \cdot \xi_{back} + \eta_5 \quad (15)$$

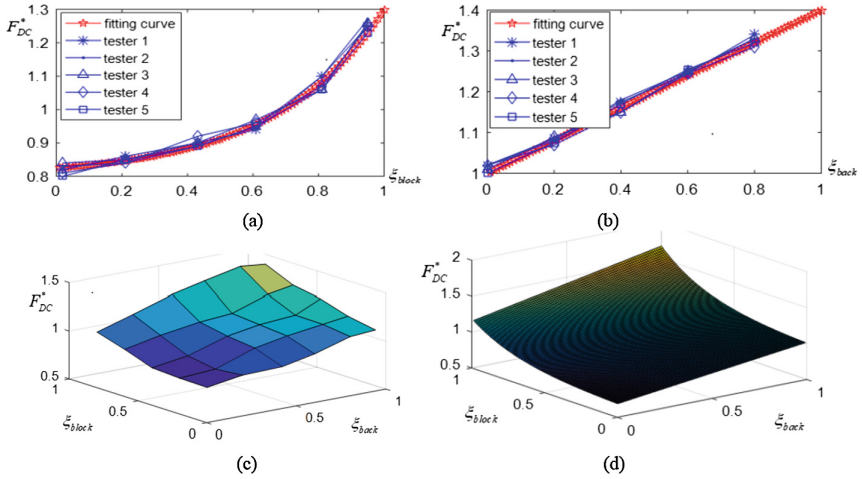


**Fig. 6.** The disorderly concealment effect factor model: (a)  $F_{DC}^*$  versus  $\xi_{block}$  in the case of  $\xi_{back} = 0$ ; (b)  $F_{DC}^*$  versus  $\xi_{back}$  in the case of  $\xi_{block} = 0$ ; (c) the measured  $F_{DC}^*$  values with different combinations of  $\xi_{block}$  and  $\xi_{back}$ ; (d) the proposed  $F_{DC}$  model with  $\xi_{block}$  and  $\xi_{back}$ .

## 5 Experimental Result

To demonstrate the effectiveness of the proposed DCT-JND profile, the ability of hiding distortion of our DCT-JND model is verified. The disorderly concealment effect factor is incorporated into our DCT-JND model and is used to adjust the conventional DCT-JND threshold. Noise is added to each DCT coefficient in an image according to [7] such as



$$C'(n, i, j) = C(n, i, j) + S_r(n, i, j) \times J(n, i, j) \quad (16)$$

where  $C(n, i, j)$  is the  $(i, j)$ -th DCT coefficient in the  $n$ -th block.  $C'(n, i, j)$  is the coefficient with the noise and  $S_r(n, i, j)$  is a bipolar random noise of  $\pm 1$ . The PSNR is used to measure the capability toleration of the JND models. With the same perceptual quality, the lower PSNR is, the more accurate the JND model is. Meanwhile, we adopt the Blind/Referenceless Image Spatial Quality Evaluator (BRISQUE) [13] as our object quality assessment to evaluate the original and distorted images. It is believed that the BRISQUE metric is more conforming to the visual characteristics of human eyes than the PSNR and SSIM [14]. It is worth pointing out that the BRISQUE score is smaller, the perceptual quality of the image is better. As we all know, good performance for a JND profile means that the distorted image by the JND profile shows a low PSNR with the smaller BRISQUE score against other compared JND profiles.

In our performance test, the images chosen from TID 2013 database are shown in Fig. 7. The proposed JND profile is compared to three recently developed JND profiles, Bae (17)'s [7], Wu (13)'s [9], Wu (17)'s [11] in performance. Bae (16)'s JND profile is a DCT-JND profile, Wu (13)'s and Wu (17)'s JND profiles are the pixel-JND models. To prove the necessity of taking into account the disorderly concealment effect, we also test the performance of the original JND profile (Original) which does not incorporate the disorderly concealment effect. Table 2 shows the performance comparison between the four recently developed JND profiles and the proposed in terms of PSNR, and RPISQUE SCORE. The average PSNR result shows that the proposed JND profile has the smallest PSNR values. Specifically, the average PSNR value of the proposed JND profile is 1.633 dB, 1.202 dB and 6.637 dB smaller than Original, Bae (17)'s and Wu (17)'s model, respectively. The BRPISQUE SCORE also denotes that the proposed JND profile shows good performance in objective quality assessment. The average BRPISQUE SCORE of Bae (17)'s model and the proposed is approximately equal. Therefore, the proposed JND profile can hide more distortions with same perceptual quality than other JND profile.



**Fig. 7.** Thumbnail of images ( $T_1, T_2, \dots, T_9$ ) set for testing.

**Table 2.** The performance comparisons in TID 2013 database

Image	PSNR (dB)					BRPISQUE SCORE				
	Original	Bae (17)'s	Wu (13)'s	Wu (17)'s	Proposed	Original	Bae (17)'s	Wu (13)'s	Wu (17)'s	Proposed
T <sub>1</sub>	29.654	29.193	31.056	34.903	28.111	84.810	84.720	154.944	96.988	85.135
T <sub>2</sub>	29.797	29.749	30.436	33.766	28.290	76.545	77.168	147.245	42.102	79.928
T <sub>3</sub>	28.401	27.963	30.430	34.612	26.474	92.074	92.445	114.389	52.292	92.246
T <sub>4</sub>	27.509	26.732	30.946	33.526	25.940	85.353	86.447	125.143	33.209	85.514
T <sub>5</sub>	27.706	27.263	30.498	32.275	26.030	88.806	88.739	90.466	24.723	88.387
T <sub>6</sub>	27.453	27.181	30.259	32.841	25.704	81.522	80.932	106.355	23.813	78.970
T <sub>7</sub>	28.077	27.396	29.789	34.253	26.916	82.112	83.675	153.689	163.577	83.209
T <sub>8</sub>	26.955	26.588	28.484	32.323	24.905	84.637	83.841	85.781	25.144	84.178
T <sub>9</sub>	28.266	27.870	31.319	35.233	26.753	81.018	81.149	172.279	63.000	84.640
Average	28.202	27.771	30.357	33.748	26.569	84.097	84.346	127.810	58.316	84.689

Figure 7 shows the subjective performance comparison of four JND profiles for ‘T1’ image. In generally, the proposed JND model has lowest PSNR value with the better perceptual quality. Bae’s JND model shows poor performance in edge region (region A). The contrast intensity calculated by SCI metric is higher relatively in edge area, which the JND threshold in this region is overestimated. Wu (13)’s JND model overestimates the visibility threshold of the smooth region. Compared with our model, Wu (17)’s JND model has highest PSNR value with the similar perceptual quality (Fig. 8).

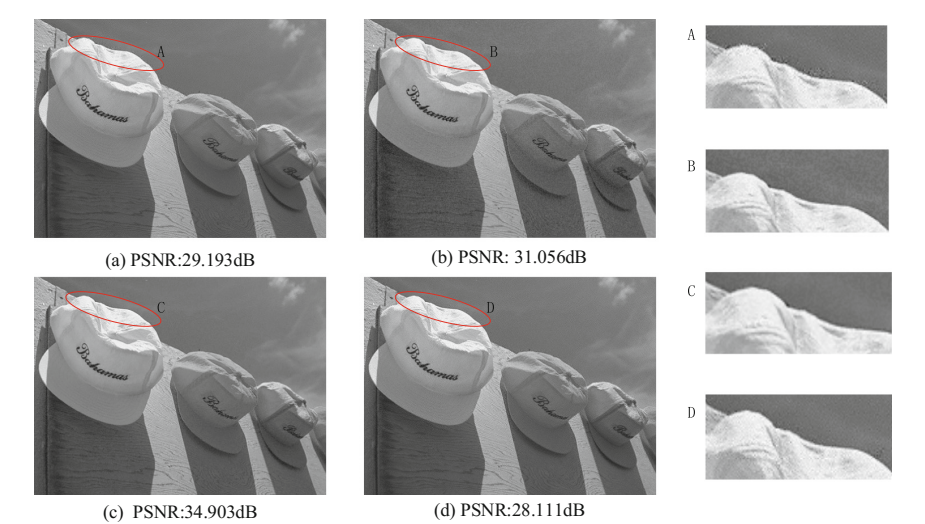


**Fig. 8.** The performance comparisons of four JND profiles: (a) by Bae (17)’s JND model; (b) by Wu (13)’s JND model; (c) by Wu (17)’s JND model; (d) by the proposed JND model.

## 6 Conclusion

In this paper, considering the disorderly concealment effect, a novel DCT-JND model was proposed. The proposed disorderly concealment effect factor was used to improve the accuracy of DCT-JND model, as an attempt for overcoming the major shortcoming of the existing DCT-JND models. In particular, the block-level disorder metric was designed to evaluate the disorder intensity of the stimulus. In order to avoid to overestimate the visibility threshold in orderly region and underestimate that of the disorderly region, we have built a disorderly concealment effect factor based on the disorder of the stimulus to adjust the conventional DCT-JND threshold appropriately. The experimental result shows that the proposed model is better in PSNR reduction with the same perceptual quality compared with existing JND profiles.

**Acknowledgement.** This work was supported in part by National Natural Science Foundation of China (NSFC) (No. 61231010) and National High Technology Research and Development Program (No.2015AA015901).

## References

1. Bae, S.-H., Kim, J., Kim, M.: HEVC-based perceptually adaptive video coding using a DCT-based local distortion detection probability model. *IEEE Trans. Image Process.* **25**(7), 3343–3357 (2016)
2. Wang, H., et al.: MCL-JCV: a JND-based H.264/AVC video quality assessment dataset. In: *Proceedings of IEEE*, pp. 1509–1513. Phoenix (2016)
3. Ritschel, T., Smith, K., Ihrke, M., Grosch, T., Myszkowski, K., Seidel, H.-P.: 3D unsharp masking for scene coherent enhancement. *ACM Trans. Graph.* **27**(3), 90:1–90:8 (2008)
4. Ahumada Jr., A.J., Peterson, H.A.: Luminance-model-based DCT quantization for color image compression. *Proc. SPIE* **1666**, 365–374 (1992)
5. Watson, A.B.: DCTune: a technique for visual optimization of DCT quantization matrices for individual images. In: *Sid International Symposium Digest of Technical Papers*, vol. 24, p. 946 (1993)
6. Wan, W., Wu, J., Xie, X., Shi, G.: A novel just noticeable difference model via orientation regularity in DCT domain. *IEEE Access* **5**, 22953–22964 (2017)
7. Bae, S., Munchurl, K.: A DCT-based total JND profile for spatiotemporal and foveated masking effects. *IEEE Trans. Image Process.* **27**(6), 1196–1207 (2017)
8. Wu, J., Shi, G., Lin, W., Liu, A., Li, F.: Pattern masking estimation in image with structural uncertainty. *IEEE Trans. Image Process.* **22**(12), 4892–4904 (2013)
9. Wu, J., Lin, W., Shi, G., Wang, X., Qi, F.: Just difference estimation for images with free-energy principle. *IEEE Trans. Image Process.* **15**(7), 1705–1710 (2013)
10. Wei, Z., Ngan, K.N.: Spatio-temporal just noticeable distortion profile for grey scale image/video in DCT domain. *IEEE Trans. Circ. Syst. Video Technol.* **19**(3), 337–346 (2009)
11. Wu, J., Li, L., Dong, W., Shi, G., Lin, W., Jay Kuo, C.-C.: Enhanced just noticeable difference model for images with pattern complexity. *IEEE Trans. Image Process.* **26**(6), 2682–2693 (2017)

12. Ojala, T., Valkealahti, K., Oja, E., et al.: Texture discrimination with multidimensional distributions of signed gray level differences. *Pattern Recognit.* **34**(3), 727–739 (2001)
13. Mittal, A., Moorthy, A.K., Bovik, A.C.: No-reference image quality assessment in the spatial domain. *IEEE Trans. Image Process.* **21**(12), 4695–4708 (2012)
14. Wang, Z., Bovik, A.C., Sheikh, H.R., Simoncelli, E.P.: Image quality assessment: from error visibility to structural similarity. *IEEE Trans. Image Process.* **13**(4), 600–612 (2004)